OPEN ACCESS

University of BRISTOL

Kynaston, E. L., Nazemi, A., MacFarlane, L. R., Whittell, G. R., Faul, C. F. J., & Manners, I. (2018). Uniform Polyselenophene Block Copolymer Fiberlike Micelles and Block Co-micelles via Living Crystallization-Driven Self-Assembly. *Macromolecules*, *51*(3), 1002-1010. https://doi.org/10.1021/acs.macromol.7b02317

Peer reviewed version

Link to published version (if available):
10.1021/acs.macromol.7b02317

Link to publication record in Explore Bristol Research
PDF-document

This is the author accepted manuscript (AAM). The final published version (version of record) is available online via ACS at https://pubs.acs.org/doi/10.1021/acs.macromol.7b02317. Please refer to any applicable terms of use of the publisher.

University of Bristol - Explore Bristol Research
General rights

This document is made available in accordance with publisher policies. Please cite only the published version using the reference above. Full terms of use are available:
http://www.bristol.ac.uk/red/research-policy/pure/user-guides/ebr-terms/

Uniform Polyselenophene Block Copolymer Fiber-like Micelles and Block Co-micelles via Living Crystallization-Driven Self-Assembly

Emily L. Kynaston,[1] Ali Nazemi,[1] Liam R. MacFarlane, George R. Whittell, Charl F. J. Faul, and Ian Manners*

Department of Chemistry, University of Bristol, Cantock's Close, Bristol, BS8 1TS, UK

[1]These authors contributed equally to this work

Table of Contents

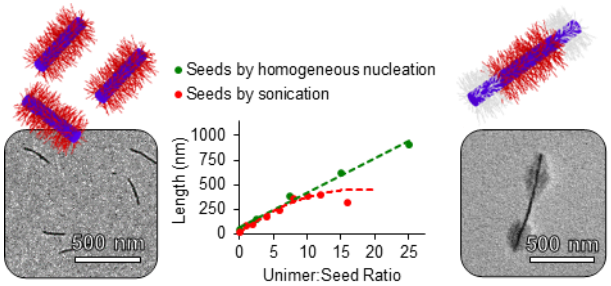

Abstract

We report the formation of near uniform block copolymer fiber-like micelles of controlled length with a crystalline polyselenophene core via the seeded growth process termed living crystallization-driven self-assembly (CDSA). Poly(3-decylselenophene)-*block*-poly(dimethylsiloxane) (P3DSe-*b*-PDMS) forms long, fiber-like micelles in selective solvents. Attempts to control the length of these fibers, by seeded growth following sonication to form the seeds, afforded samples with lengths limited to ca. 300 nm. However, we found that direct dispersion of P3DSe-*b*-PDMS in diethyl ether yields short and relatively low dispersity nanofibers (L_n = 41 nm; L_w/L_n = 1.16) which can be used as seeds. In this case,

seeded growth led to low dispersity fibers with length control up to ca. 900 nm. Moreover, we demonstrate that block co-micelles with spatially distinct PDMS and polystyrene (PS) coronal segments can be accessed from the sequential addition of dissolved P3DSe-*b*-PS to preformed P3DSe-*b*-PDMS micelles.

Introduction

The solution self-assembly of synthetic amphiphiles such as block copolymers (BCPs) represents a powerful route to nanoparticles (or micelles) based on soft matter. As a result of the compositional flexibility arising from state-of-the-art synthetic methods, the resulting colloidal nanostructures have broad variety of properties and potential applications.[1–6] However, control of their dimensions and segmentation, especially for non-spherical assemblies, generally represents a substantial challenge. A series of studies have demonstrated that the use of a BCP with a crystallizable core-forming block can enable the use of efficient seeded-growth procedures whereby uniform one-dimensional (1D) fibers[7–12] or two-dimensional (2D) platelet morphologies[13–16] can be formed. Segmented "block co-micelle" and other complex architectures can be prepared by sequential addition of different BCPs to short, seed micelles.[9–11] These processes have been termed "living" crystallization-driven self-assembly (CDSA) in analogy to living covalent polymerization of monomers. Living CDSA-type seeded growth approaches have also been shown to be valid for supramolecular polymers under conditions of suppressed dynamic exchange to allow access to uniform and complex assemblies.[17–25]

π-Conjugated polymers are promising candidates for uses in organic electronic and optoelectronic devices and can be fabricated into nanowires for nanoelectronic applications.[26,27] BCPs with a crystallizable π-conjugated block are readily accessible and their assembly into fiber-like micelles with a crystalline core has been well-established.[28–40]

We have previously shown that living CDSA procedures can be applied to poly(3-hexylthiophene) (P3HT) BCPs to afford fibers of controlled length and also block co-micelles.[41–43] This type of self-assembly has also recently been achieved with poly(phenylene vinylene) BCPs, thus expanding the scope of π-conjugated polymers capable of living CDSA.[44] Moreover, uniform fibers fabricated by living CDSA containing such semiconducting π-conjugated polymers have been incorporated as the active layer in field-effect transistors. The resulting mobilities are dependent on fiber length and the degree of polymerization of the P3HT core block, providing routes to tuneable functionality in such devices.[45]

In this paper we report on our attempts to apply living CDSA protocols to polyselenophene BCPs. Polyselenophenes are selenium-containing analogues of the ubiquitous polythiophenes and have been developed into an important class of π-conjugated polymers. They exhibit desirable properties for organic electronics including a lower band-gap than their polythiophene analogues,[46,47] which is a requirement for efficient harvesting of solar energy for photovoltaic applications.[26,27,48] Polyselenophenes have also been shown to possess different crystallization properties to polythiophenes, arising from significant interchain Se-Se interactions,[49] and therefore may exhibit distinct living CDSA behaviour.

Results and Discussion

(i) Synthesis and Characterization of P3DSe-*b*-PDMS

We have previously shown that poly(3-heptylselenophene) (P3C7Se) copolymers with an amorphous polystyrene (PS) block are able to form long nanofibers with semicrystalline P3C7Se cores in solvents selective for the PS block by CDSA.[50] However, our attempts to gain length control of these nanofibers using living CDSA techniques were inhibited by low solubility of the poly(3-heptylselenophene) (P3C7Se) segment and strong

propensity of the PS block to aggregate. Consequently, for the living CDSA studies described herein we used poly(3-decylselenophene) (P3DSe) as the crystallizable segment which has enhanced solubility relative to P3C7Se. Poly(dimethylsiloxane) (PDMS) was selected as the corona-forming block as previously PDMS co-blocks have been used successfully in the self-assembly of both polythiophene and polyselenophene BCPs.[43,50] Furthermore, micelles with PDMS coronas do not tend to aggregate as strongly as those with alternative hydrophobic shells such as PS.[9,43] For these studies, catalyst transfer polycondensation and copper-catalyzed azide-alkyne cycloaddition (CuAAC) reactions were used to synthesize poly(3-decylselenophene)-*block*-poly(dimethylsiloxane) ($P3DSe_{17}$-*b*-$PDMS_{240}$) (where subscripts denote degree of polymerization) (Scheme 1). The 2,5-dibromo-3-decylselenophene monomer (**1**) was synthesized from a Weinreb amide precursor as previously published elsewhere.[51–53] The catalyst transfer polycondensation of **1** and subsequent quenching with ethynylmagnesium bromide yielded **2** with moderate degrees of alkyne end-capping as has previously been reported for end-capped polythiophenes.[54] The number-average molecular weight (M_n = 4600 g mol^{-1}) of **2** and degree of alkyne end-capping (44 %) were ascertained by matrix-assisted laser desorption ionisation time-of-flight (MALDI-TOF) mass spectrometry on the homopolymer (Figure S2). The low degree of alkyne end-capping in comparison to polythiophenes[54] was attributed to the lower solubility of P3DSe.

Living anionic polymerization of hexamethylcyclotrisiloxane and quenching with an excess of (bromomethyl)chlorodimethylsilane afforded bromo-terminated $PDMS_{240}$. As PDMS has a similar refractive index to THF, the gel permeation chromatography (GPC) trace was relatively weak in intensity (Figure S3). However, we were able to extract a value for polydispersity ($Đ$ = 1.12) using this technique. The number-average molecular weight of PDMS (17,800 g mol^{-1}) was calculated from integration of the *n*-butyl proton peaks (δ = 1.32, 0.88 and 0.53 ppm) relative to the methyl proton peak (δ = 0.08 ppm) in the ^{1}H-NMR

spectrum (Figure S4). The degree of bromo-functionalization (> 99 %) was determined by integration of the methylene proton peak adjacent to the end-group (δ = 2.43 ppm) relative to the *n*-butyl proton peaks. The bromo end-group was subsequently converted to an azide in THF using sodium azide and tetrabutylammonium bromide as a phase-transfer reagent. Complete conversion of the bromo group to the azido group was characterized by a downfield shift in the end-group methylene proton peak (δ = 2.74 ppm) in the ^{1}H-NMR spectrum (Figure S5). As the P3DSe$_{17}$ homopolymer was not 100 % alkynyl-capped, a slight (ca. 1.2 mol%) excess of **2** was used for the CuAAC reaction. Preparative size exclusion chromatography (SEC) was used to remove any residual P3DSe$_{17}$ homopolymer from the resulting P3DSe$_{17}$-*b*-PDMS$_{240}$, which was isolated as a purple gum. The polydispersity (*Đ* = 1.04) of the purified material was determined by GPC analysis (Figure S7).

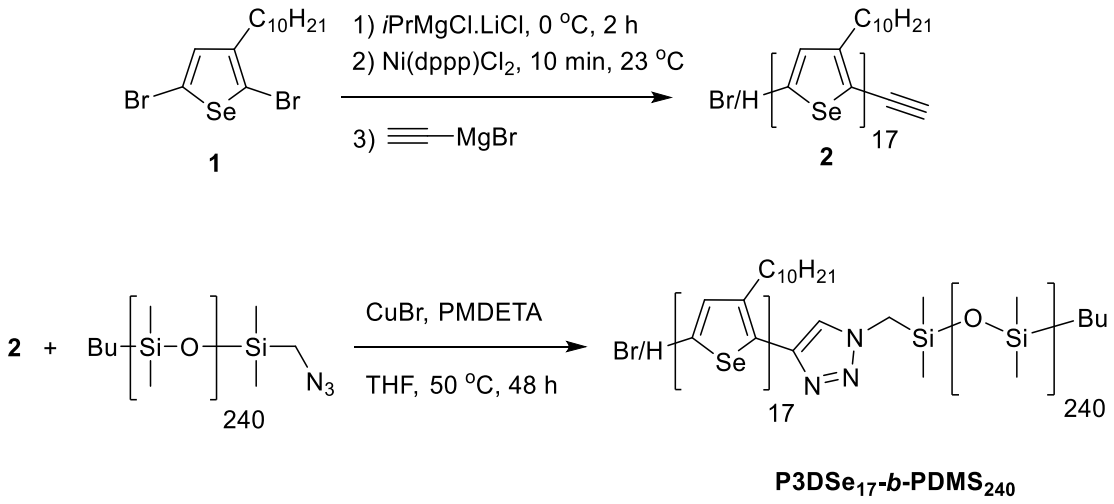

Scheme 1. Synthesis of P3DSe-*b*-PDMS by the CuAAC of alkyne-terminated P3DSe (**2**) and azido-PDMS. PMDETA = *N,N,N′,N″,N″*-pentamethyldiethylenetriamine.

(ii) Attempted Living CDSA of P3DSe$_{17}$-*b*-PDMS$_{240}$ Using Seeds Formed by Sonication in Ethyl Acetate

Self-assembly of P3DSe$_{17}$-*b*-PDMS$_{240}$ was initially investigated in ethyl acetate (EtOAc), a selective solvent for PDMS (Scheme 2). The BCP was suspended in EtOAc at room temperature (23 °C), heated to 70 °C for 1 h then allowed to cool back to ambient temperature. This resulted in the formation of long, fiber-like micelles, the cores of which had sufficient electron contrast to be visualized by transmission electron microscopy (TEM) imaging (after solvent evaporation) without the need for staining (Figure 1a). Analysis of the fibers gave an average core width of 7.4 ± 1.4 nm which is in good agreement with the expected theoretical length of 6.7 nm based on a fully extended chain with repeat unit lengths of 0.392 nm.[55]

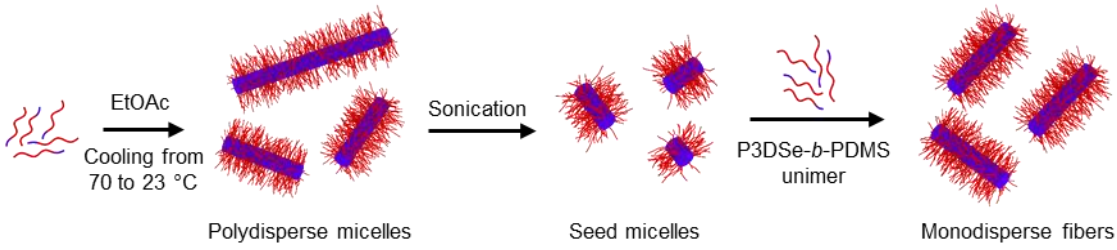

Scheme 2. Schematic representation of the preparation of P3DSe$_{17}$-*b*-PDMS$_{240}$ BCP fibers by seeded growth of unimer from seeds formed by sonication of polydisperse micelles.

Wide-angle X-ray scattering (WAXS) measurements on a dried sample of polydisperse fibers was inconclusive with regards to core crystallinity as the expected peaks corresponding to the P3DSe block interlayer spacing and π-stacking were not visible above the baseline (Figure S8). As the presence of crystallinity was supported by UV-Vis data (vide infra) we attribute this to the low volume fraction of the crystallizable P3DSe block relative to the amorphous PDMS. This volume fraction is much smaller than that for a previously reported sample of polyselenophene BCP fiber-like micelles for which WAXS analysis was successful. Similar measurements on a sample of P3DSe$_{17}$ homopolymer revealed sharp

reflections indicative of crystalline packing superimposed on a broad amorphous halo (Figure S9). The (100) reflection associated with the interlayer distance was observed at 17.1 Å along with higher order reflections at 8.6 Å (200) and 4.1 Å (300). The (010) π-π stacking reflection was observed at 3.2 Å. Typically, only (100) and (010) and the associated higher order reflections are observed by WAXS for the Type 1 polymorph of poly(3-hexylthiophene).[56] The additional reflection observed at 4.6 Å is associated with alkyl chain tilting, commonly noted in Type 2 polymorphs, which have been observed in pure form in polyselenophenes and mixed phases in longer side chain poly(3-alkylthiophene)s.[49,57] The large amorphous halo was attributed to disordered regions of aggregated polymer chains, as the sample was not annealed, in addition to scattering from the silicon substrate.

The presence of crystallinity in the cores of the P3DSe$_{17}$-*b*-PDMS$_{240}$ micelles was confirmed in solution by UV/Vis absorption spectroscopy. The UV/Vis spectrum of the P3DSe$_{17}$-*b*-PDMS$_{240}$ unimer in THF (0.02 mg/mL) showed an absorption maximum (λ_{abs}) of 450 nm with a very small, low-energy vibronic band (600 nm) which might be accounted for by the presence of a small degree of aggregation in THF (Figure S10). The measured λ_{abs} in THF was hypsochromically-shifted relative to similar P3C7Se BCPs ($\lambda_{abs} \approx 480$ nm in THF) which could be due to backbone torsion in P3DSe to minimize steric repulsion between the longer alkyl chain substituents.[58] UV/Vis absorption spectra of the micelles in EtOAc (0.02 mg/mL) showed a red shifted spectrum (λ_{abs} = 500 nm) with a significant low-energy vibronic feature at 575 nm indicative of planarization of the P3DSe chains (Figure S10).[59] Furthermore, the photoluminescence spectrum of the P3DSe$_{17}$-*b*-PDMS$_{240}$ micelles in EtOAc (λ_{em} = 570 nm; 0.02 mg/mL) showed the expected aggregation-induced fluorescence quenching (ca. 70 % quenched) relative to the BCP unimer in THF (λ_{em} = 560 nm; 0.02 mg/mL) (Figure S11).[60] The red-shift (ca. 50 nm) between BCP unimer in THF and micelles in EtOAc in the optical absorption spectra may be indicative of polymorphism in the BCP

micelle, crystalline cores as λ_{abs} is around 500 nm for the type-2 structure in thin films of poly(3-hexylselenophene).[49]

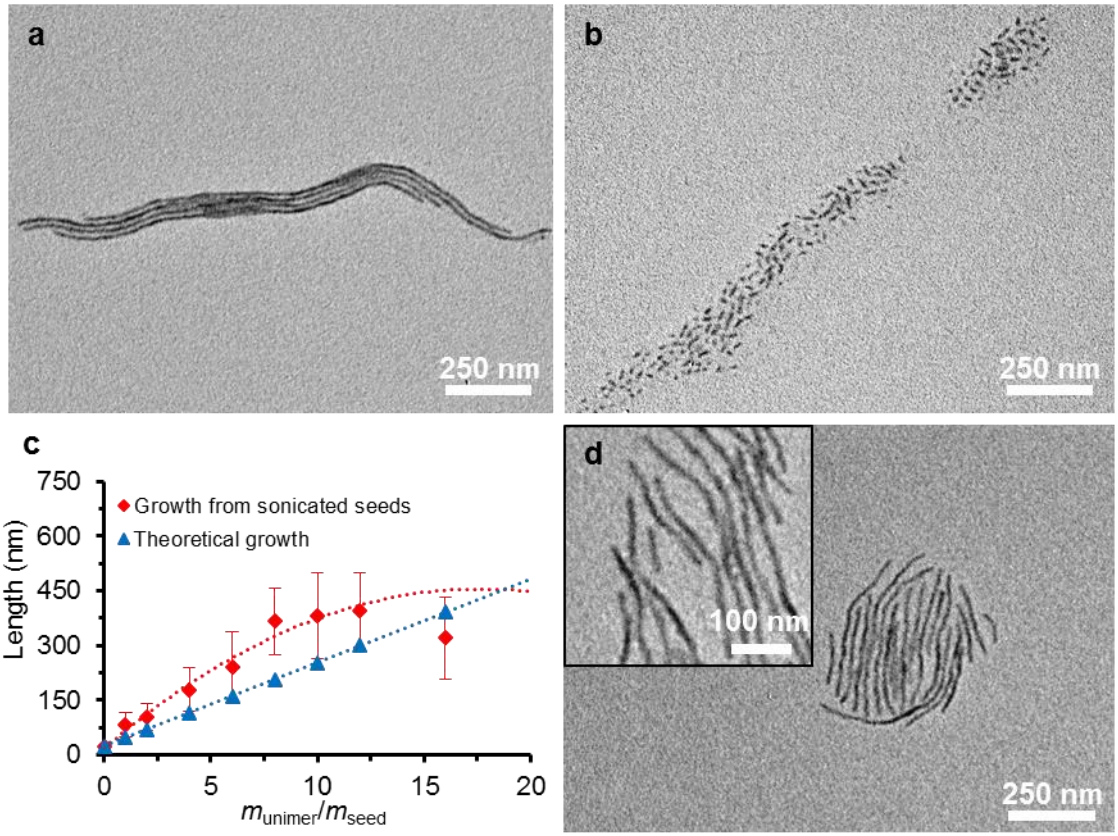

Figure 1. Bright-field TEM images of P3DSe$_{17}$-*b*-PDMS$_{240}$ in EtOAc (a) before and (b) after ultrasonication. (c) Plot of experimentally obtained micelle length (L_n) and theoretical length at different m_{unimer}/m_{seed} mass ratios. (d) Micelles obtained after addition of 16 unimer equivalents, inset highlighting increased polydispersity.

Living CDSA of BCPs with crystallizable core-forming blocks is most commonly achieved by ultrasonication of long, polydisperse 1D precursor micelles followed by the addition of further BCP unimers to the seeds. An alternative approach involves thermal or solvent annealing of short micelles formed by sonication, a process termed self-seeding.[61,62] Ultrasonication of the long P3DSe$_{17}$-*b*-PDMS$_{240}$ micelles in EtOAc yielded short (ca. 20 nm), low dispersity (L_w/L_n = 1.06) seeds (Figure 1b). However, attempts to perform living CDSA

by the addition of P3DSe$_{17}$-*b*-PDMS$_{240}$ unimer in THF to the seeds in EtOAc (mass ratios, m_{unimer}/m_{seed}, ranging from 1 to 16) were met with limited success. Although growth from the seed termini was apparent by TEM analysis (Figure 1d), the length of fibers prepared using this technique was limited to ca. 300 nm. Addition of BCP unimer to the seed fibers resulted in an increase in fiber length dispersity (L_n/L_w) from 1.06 to between 1.12 and 1.18. Furthermore, deviation of the experimentally obtained length from theoretical fiber length, obtained by assuming a constant number of chains per unit length, suggests that growth from all seeds is not uniform (Figure 1c). Above 10 equivalents of unimer, homogeneous nucleation was favoured over epitaxial growth from the fiber ends, resulting in a decrease in average length (L_n). Competing homogeneous nucleation was previously identified in our studies of the seeded growth of fiber-like P3HT BCP micelles with a poly(methyl methacrylate) corona[63] and a similar problem in terms of growth from seeds generated by sonication has been noted for the cases of P3HT-*b*-PDMS and P3HT-*b*-P2VP.[41,42] We also attempted to prepare uniform fibers by self-seeding[61,62] of the short, P3DSe$_{17}$-*b*-PDMS$_{240}$ seed micelles prepared by ultrasonication of long fibers, a procedure that has been successful in the case of P3HT BCPs.[43,45] However, heating to just below their apparent dissolution temperature (determined as the maximum temperature at which no significant colour change was observed from purple to red associated with disruption of the molecular packing of the P3DSe chain)[47] and subsequent cooling to room temperature was also met with limited success and polydisperse micelles were observed by TEM after solvent evaporation (Figure S12).

As discussed previously in the case of P3HT analogues,[41,42] the failure to achieve lengths beyond ca. 300 nm using living CDSA of P3DSe$_{17}$-*b*-PDMS$_{240}$ is likely to be a consequence of the introduction of crystalline defects to the seeds during their formation by ultrasonication. Presumably, these defects lead to a defect amplification effect as the seed

micelles elongate through unimer deposition at the termini, which eventually results in further growth being completely curtailed. Chemical defects caused by ultrasonication, such as chain cleavage, have been ruled out by GPC studies which show no significant change in molar mass or dispersity after sonication of self-assembled structures (Figure S13).

(iii) Living CDSA of P3DSe$_{17}$-*b*-PDMS$_{240}$ Using Seeds Formed by Direct Dissolution in Diethyl Ether

To address the aforementioned limitations, we turned our attention to the generation of seed micelles under conditions that would not require sonication (Figure 2a) and might therefore be anticipated to contain fewer defects. Our preliminary self-assembly experiments in a variety of PDMS-selective solvents (including hexanes, decane, EtOAc, and *n*-butyl acetate) indicated that P3DSe$_{17}$-*b*-PDMS$_{240}$ formed short (L_n < 50 nm), relatively uniform micelles only when directly dispersed in diethyl ether (Et_2O) at ambient temperature. Heating was required to dissolve the polymer in the other solvents and the fibers formed were long and polydisperse, as is typical for their formation by a homogeneous nucleation mechanism. It appears that Et_2O is slightly better at solvating the crystallizable P3DSe block relative to the other hydrophobic solvents so that the material dissolves. However, this solvent medium must also be sufficiently poor for P3DSe that homogeneous nucleation is unusually efficient so that short micelles are formed. Similar results have been observed in other cases where direct dissolution in a medium of poor solvent quality for the core-forming block yields shorter micelles.[64–66] In a typical experiment, direct dissolution of the BCP in Et_2O at ambient temperature (23 °C) yielded short fibers with an average length of 41 nm and relatively narrow length distribution by TEM (L_w/L_n = 1.16) (Figure 2b and 2c). As sonication was not used for their formation, the possibility of using these short micelles as alternative seeds for living CDSA of the P3DSe$_{17}$-*b*-PDMS$_{240}$ BCP was explored.

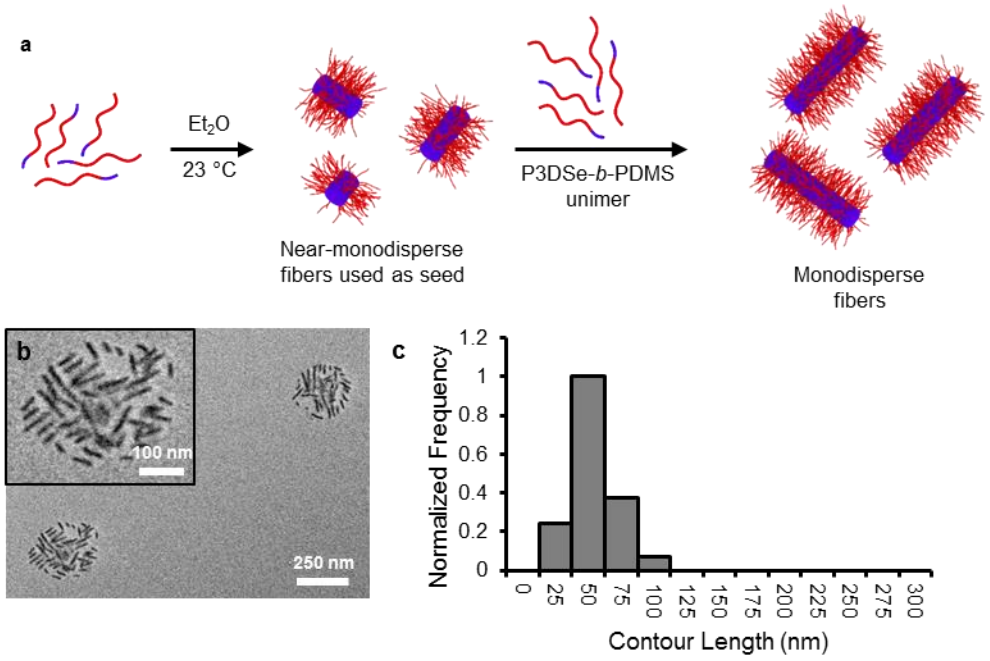

Figure 2. (a) Schematic representation of the preparation of near monodisperse P3DSe$_{17}$-*b*-PDMS$_{240}$ BCP fibers; (b) Bright-field TEM micrograph of micelles prepared by direct dissolution of the BCP in Et_2O at room temperature (L_n = 41 nm, L_w/L_n = 1.16); (c) Histogram of the contour length distribution of seeds in (b). The scale on the x-axis is offset by a value of 25 nm for clarity.

These seed micelles were then used for seeded growth experiments using P3DSe$_{17}$-*b*-PDMS$_{240}$ BCP unimer solution. To favour the formation of near monodisperse fibers of controlled length, the short (L_n = 41 nm) P3DSe$_{17}$-*b*-PDMS$_{240}$ seeds in Et_2O were first diluted (with EtOAc) in separate vials. To further suppress homogeneous nucleation of the BCP, the THF content was adjusted to 20% (v/v) in all the samples. Different amounts of P3DSe$_{17}$-*b*-PDMS$_{240}$ were then added as a solution in THF to these vials. The resulting mixtures were aged for 2 days at room temperature. TEM analysis of the samples revealed the presence of elongated micelles with lengths that correlated linearly with the unimer to seed ratio (Figure 3a-d). Using this protocol the formation of P3DSe$_{17}$-*b*-PDMS$_{240}$ nanofibers of controlled lengths up to ca. 900 nm with narrow length distributions (L_w/L_n < 1.20) were successfully

achieved (Figure 3f). Comparison of the theoretical micelle length, obtained by assuming a constant number of chains per unit length, with the experimentally measured length shows only slight deviation, indicating successful epitaxial growth of the added BCP unimer onto the seed micelles (Figure 3e).

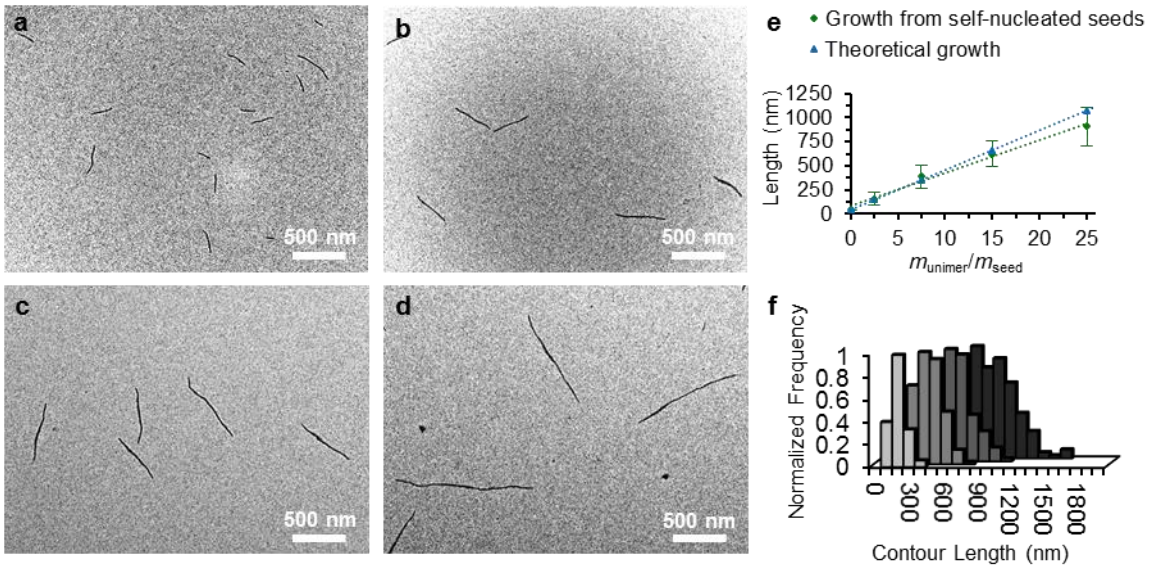

Figure 3. TEM micrographs of P3DSe$_{17}$-*b*-PDMS$_{240}$ fibers grown from P3DSe$_{17}$-*b*-PDMS$_{240}$ seed micelles (L_n = 41 nm) with m_{unimer}/m_{seed} of 2.5:1 (a), 7.5:1 (b), 15:1 (c), and 25:1 (d). (e) Plot showing experimentally obtained fiber length (L_n) and theoretical lengths based on different m_{unimer}/m_{seed} mass ratios. (f) Histogram showing the contour length distribution of fibers with m_{unimer}/m_{seed} of 2.5:1, 7.5:1, 15:1, and 25:1 (front to back, respectively).

(iv) Formation of Block Co-Micelles with a P3DSe Core

In addition to uniform 1D assemblies, living CDSA provides a controlled route to complex architectures such as segmented micelles via the sequential addition of BCPs with different corona-forming blocks to the seeds.[7,9,15] To explore the formation of block co-micelles with a polyselenophene core we synthesized another P3DSe BCP with a hydrophobic PS coronal block using a similar CuAAC reaction between azido-PS and

alkyne-terminated P3DSe (Scheme S1, Figures S14-18).[43] To obtain triblock co-micelles, P3DSe$_{17}$-*b*-PS$_{140}$ unimer in THF was added to P3DSe$_{17}$-*b*-PDMS$_{240}$ fibers (L_n = 390 nm, L_w/L_n = 1.10) which had been diluted in EtOAc (0.12 mg/mL) (Figure 4a). After aging for 2 days, B-A-B triblock co-micelles with distinct coronal segments were visible by TEM without the need for staining (Figure 4b-e), due to the inherent higher electron density of PS relative to the central PDMS segment. The solvent composition was modified in order to ensure a 20% (v/v) THF content to minimize the homogeneous nucleation of the P3DSe$_{17}$-*b*-PS$_{140}$ BCP upon its addition. As can be observed in Figure 4b, these micelles were strongly aggregated after solvent evaporation. This behaviour was attributed to the tendency for PS coronal blocks to aggregate, which has been reported in several studies.[9,43,50] However, distinct micelle segments with different widths were clearly observable in the aggregates as indicated by the arrows. In addition, end-to-end coupled (Figure 4c) and isolated block co-micelles (Figure 4d, e) as well as aggregates were imaged in the same sample. Unfortunately, the extent of the aggregation hindered our ability to perform statistical length analysis.

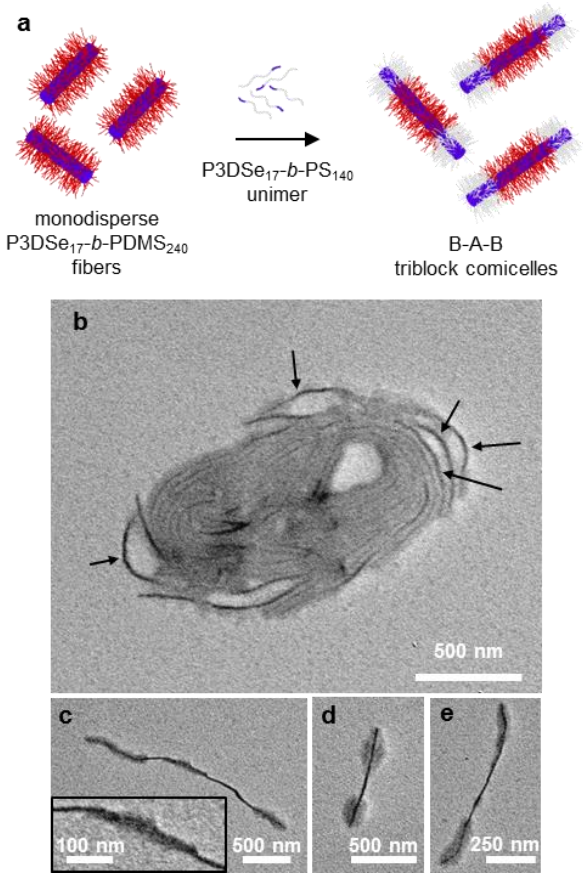

Figure 4. (a) Schematic representation of the formation of B-A-B block co-micelles. b-e) Bright-field TEM images of B-A-B (P3DSe$_{17}$-*b*-PS$_{140}$)-*m*-(P3DSe$_{17}$-*b*-PDMS$_{240}$)-*m*-(P3DSe$_{17}$-*b*-PS$_{140}$) triblock co-micelles. Arrows in (b) point to the observable block co-micelles within the micellar aggregate. (c) End-to-end coupling of block co-micelles, which presumably occurs as a result of intermicelle PS coronal interactions. The region of overlap is shown at a higher magnification in the inset. (d, e) Isolated block co-micelles in the same sample.

Summary

A route to efficiently perform living CDSA of amphiphilic polyselenophene BCPs has been developed. By preparing short seed micelles (L_n < 50 nm) from the direct dispersion of P3DSe$_{17}$-*b*-PDMS$_{240}$ in Et$_2$O under ambient conditions where homogeneous nucleation is favoured, the use of ultrasonication, which is believed to cause seed defects, can be

circumvented. This allowed near-uniform micelles of controlled lengths up to ca. 900 nm to be obtained. Furthermore, addition of a second P3DSe BCP with a PS corona-forming block to fibers of P3DSe$_{17}$-*b*-PDMS$_{240}$ yields B-A-B block co-micelles with distinct PDMS and PS coronal segments. These B-A-B segmented structures were resolvable by TEM through their inherent electron density contrast.

Although the seeds required for living CDSA processes can often be successfully generated by sonication of longer micelles,[67] difficulties are encountered in some cases where the core- or corona-forming blocks can undergo undesirable side reactions. The approach involving the formation of seed micelles by direct dissolution in a poor solvent for the core may be broadly applicable to BCPs with crystallizable core-forming blocks that are sensitive to sonication. Further studies aimed at investigating the influence of sonication on the seeds and establishing the generality of this new approach which, in principle, is simpler than the use of self-seeding approaches to control fiber length,[43,45,61,62] are in progress. A detailed investigation of the properties and optoelectronic applications of the fiber-like micelles with an electroactive polyselenophene core and those of related materials is also currently underway.

Experimental Section

General Considerations

All reactions were carried out on a Schlenk line or in an MBraun glovebox under a purified nitrogen atmosphere unless otherwise stated. 2,5-Dibromo-3-decylselenophene has previously been characterized by the Heeney group and was synthesized using a modified method reported by Seferos and coworkers.[51–53] [1,3-bis(diphenylphosphino)propane] dichloronickel (Ni(dppp)Cl$_2$), isopropylmagnesium chloride lithium chloride complex (*i*PrMgCl.LiCl, 1.3 M in THF), ethynylmagnesium bromide (0.5 M in THF), styrene,

hexamethylcyclotrisiloxane (D_3), (bromomethyl)chlorodimethylsilane, tetra-*n*-butylammonium bromide ([*n*Bu_4NBr]), sodium azide (NaN_3), *N,N,N',N'',N''*-pentamethyldiethylenetriamine (PMDETA) and copper(I)bromide (CuBr) were purchased from Sigma Aldrich. All reagents were used as received unless otherwise stated. Tetrahydrofuran (THF) was purified by using alumina/copper catalyst drying deoxygenation columns from Anhydrous Engineering Inc. before use. Styrene was dried over CaH_2, distilled under reduced pressure and stored in the glovebox freezer at -40 °C prior to use. (Bromomethyl)chlorodimethylsilane was distilled prior to use. D_3 was dissolved in pentane, dried over CaH_2 for 18 h before the solvent was removed under static vacuum. D_3 was obtained by sublimation at room temperature (23 °C) under static vacuum and stored at -40 °C in the glovebox freezer. For the anionic polymerization of styrene and D_3, THF was distilled from Na/benzophenone immediately prior to use.

^{1}H-NMR spectra were obtained on a Varian 400 (^{1}H: 400 MHz) instrument at room temperature (23 °C) and referenced to residual solvent peaks in $CDCl_3$. Multi detection gel permeation chromatography (GPC) measurements were carried out at 35 °C at a flow rate of 1.0 mL min^{-1} in THF eluent on a Viscotek GPCmax equipped with both a UV-vis detector operating at 450 nm and differential refractometer. Samples were dissolved in THF (1.00 mg/mL unless otherwise stated) and filtered with a Ministart SRP 15 filters (pore size 0.45 µm) prior to analysis. Matrix-assisted laser desorption ionisation time-of-flight (MALDI-TOF) mass spectrometry measurements of homopolymers were performed using a Bruker Ultraflextreme operating in linear mode. Samples were prepared using a *trans*-2-[3-(4-*tert*-butylphenyl)-2-methyl-2-propenylidene]malononitrile matrix (75 mg/mL in $CHCl_3$) and the polymer sample (5 mg/mL in $CHCl_3$), mixed in a 10:1 (v/v) ratio. Approximately 1 µL of the mixed solution was deposited onto a stainless steel sample plate and allowed to dry in air. M_w and M_n values were extracted from the MALDI-TOF spectra using PolyTools software.

Transmission electron microscopy (TEM) was performed on a Jeol JEM 1200 EX microscope operating at 120 kV, equipped with a SIS MegaView III digital camera. Samples were prepared by drop-casting aliquots (ca. 10 μL) of the solutions onto carbon-coated copper grids which were placed on a piece of filter paper to absorb excess solvent. TEM images were analysed using ImageJ: 200-250 micelles were traced by hand to determine the contour lengths and from this data, number-averaged contour lengths (L_n) and length-averaged contour lengths (L_w) were determined from Equations (1) and (2). The distribution of micelle lengths is characterized by L_w/L_n.

$$L_n = \frac{\sum_{i=1}^{n} N_i L_i}{\sum_{i=1}^{n} N_i} \quad \textbf{(1)}$$

$$L_w = \frac{\sum_{i=1}^{n} N_i L_i^2}{\sum_{i=1}^{n} N_i L_i} \quad \textbf{(2)}$$

Wide-angle X-Ray scattering (WAXS) experiments were carried out on a D8 Advance diffractometer fitted with an 0.6 mm fixed divergence slit, knife-edge collimator and a LynxEye area detector using $Cu_{K\alpha}$ (λ = 1.54 Å). Samples were prepared by drop-casting solutions onto a silicon wafer prior to analysis. UV-vis spectra were obtained on a Shimadzu UV-2600 UV-vis spectrophotometer with an ISR-2600 integrating sphere attachment over a wavelength range of 300-1000 nm.

Ethynyl-capped P3DSe$_{17}$

2,5-dibromo-3-decylselenophene (1.00 g, 2.33 mmol) was dissolved in anhydrous THF (150 mL) in a 250 mL Schlenk flask equipped with a magnetic follower and cooled to 0 °C in an ice bath. *i*PrMgCl.LiCl complex (1.80 mL, 2.33 mmol, 1.3 M in THF) was added dropwise to the rapidly stirring solution and the GRIM reaction was left to proceed for 1 h before warming to room temperature (23 °C). Ni(dppp)Cl_2 (50.0 mg, 93.2 μmol, 4.00 mol %) was

added in one portion and polymerization, marked by a colour change from pale yellow to dark red, was allowed to proceed for 10 min before quenching with ethynylmagnesium bromide (ca 1.5 mL, 0.5 M in THF). The reaction mixture was stirred for 10 min before precipitation into MeOH (ca. 800 mL). The crude polymer mixture was isolated by pouring the suspension through a Soxhlet thimble. The polymer was purified by Soxhlet extractions in MeOH (18 h) and *n*-hexane (3 washes) before extraction into $CHCl_3$ (18 h). The solvent was removed *in vacuo* yielding P3DSe as a dark-purple solid (195 mg, 31 %). M_n and degree of end-capping were determined by MALDI-TOF: M_n = 4600 g mol^{-1}. $Đ$ = 1.06 (GPC). ^{1}H-NMR (400 MHz, $CDCl_3$) ppm δ = 7.11 (br s, aromatic, 1H), 3.49 (s, alkyne), 2.73 (t, J = 7 Hz, methylene, 2H), 1.66-1.28 (m, alkyl, 16H), 0.88 (t, J = 7 Hz, terminal alkyl, 3H).

Bromo-terminated polydimethylsiloxane (PDMS)

Hexamethylcyclotrisiloxane (1.00 g, 4.50 mmol) was dissolved in freshly distilled THF (10 mL) in a 50 mL greaseless Schlenk flask equipped with a magnetic follower. The solution was cooled to -10 °C in the glovebox. The solution was stirred rapidly and *n*BuLi (34 µL, 0.054 mmol, 1.6 M in *n*-hexane) was added in one portion. Polymerization was allowed to proceed for 18 h after which time the flask was transferred to a Schlenk line and quenched with (bromomethyl)chlorodimethylsilane (several drops transferred via canula). The bromo-terminated polymer was precipitated once into a 1:10 (v/v) Et_3N:MeOH mixture and twice into MeOH. The final product was isolated as a clear liquid by centrifugation. Yield = 920 mg, 92 %. Molecular weight was established from ^{1}H-NMR integration of the bromomethyl proton peak (δ = 2.43 ppm) and *n*-butyl proton peaks (δ = 1.32, 0.88 and 0.53 ppm) against the siloxane methyl group proton peaks (δ = 0.08 ppm, M_n = 18,900 DP_n = 240). ^{1}H-NMR (400 MHz, $CDCl_3$) ppm δ = 2.43 (s, bromo methyl, 2H), 1.31 (m, *n*-butyl, 4H), 0.88 (t, J = 7 Hz, *n*-butyl, 3H), 0.53 (t, J = 9 Hz, *n*-butyl, 2H) and 0.08 (br s, silyl methyl, 1440H).

Azido-PDMS

Bromo-terminated $PDMS_{240}$ (920 mg, 0.049 mmol) was dissolved in bench THF (10 mL) in a 50 mL greaseless Schlenk flask equipped with a magnetic stirrer bar. NaN_3 (32.5 mg, 0.50 mmol) and tetrabutylammonium bromide (161 mg, 0.50 mmol) were added and the reaction mixture was stirred at 50 °C for 48 h. Azide-terminated $PDMS_{240}$ was isolated as a clear liquid by precipitation into MeOH and centrifugation (3 times). Yield = 890 mg, 97 %. ^{1}H-NMR (400 MHz, $CDCl_3$) ppm δ = 2.74 (s, azido methyl, 2H), 1.31 (m, *n*-butyl, 4H), 0.88 (t, (m, J = 7 Hz, *n*-butyl, 3H), 0.53 (t, J = 9 Hz, *n*-butyl, 2H) and 0.08 (br s, silyl methyl, 1400H).

P3DSe$_{17}$-*b*-PDMS$_{240}$

Ethynyl-capped $P3DSe_{17}$ (15.0 mg, 3.20 µmol) and azide-terminated $PDMS_{240}$ (50.0 mg, 2.70 µmol) were dissolved in dry THF (3 mL) in a 50 mL greaseless Schlenk flask equipped with a magnetic stirrer bar. PMDETA (15 µL, 0.0001 mmol) was added and the solution was freeze-pump-thawed in liquid N_2 for 3 cycles, allowed to warm to room temperature (23 °C) and transferred to an Argon-filled glovebox. CuBr (ca. 10 mg) was added and the flask was transferred back to the Schlenk line. The reaction was allowed to proceed at 50 °C for 48 h after which time the solution was filtered through basic alumina. The crude BCP was isolated by precipitation into MeOH (3 times). The P3DSe$_{17}$-*b*-PDMS$_{240}$ BCP was isolated as a purple solid after SEC purification. Yield = 15.0 mg, 23 %. ^{1}H-NMR (400 MHz, $CDCl_3$) ppm δ = 7.11 (br s, selenophene aromatic), 2.74 (t, J = 7 Hz, selenophene methylene), 1.66-1.28 (m, selenophene alkyl), 0.88 (t, J = 7 Hz, selenophene terminal alkyl), 0.08 (br s, silyl methyl). *Đ* (GPC) = 1.04. The degree of polymerization of the P3DSe block was determined by MALDI-

TOF (Figure S2) and that of the PDMS block was determined by integration of the *n*-butyl proton peaks against the methyl proton peaks (Figure S4).

Bromo-terminated polystyrene (PS)

Sec-BuLi (75 μl, $1.05x10^{-4}$ mol) (1.4 M in cyclohexane) was added via micro syringe to a rapidly stirring solution of styrene (1.42 g, 13.7 mol) in cyclohexane (8 mL). After 90 mins, a solution of diphenylethene (28 mg, 0.158 mmol) in THF (8 mL) was added to the reaction mixture. The reaction was then cooled to -78 °C and the living polymer was quenched by dropping slowly into a solution of dibromopropane (211 mg, 1.05 mmol) in THF (8 mL). The product was isolated as a white powder by precipitation from THF into MeOH (3 times). Yield: 1.34 g (94 %). M_n 14,380 Da, M_w 16,300 Da, $Đ$ = 1.13 (GPC). ^{1}H-NMR (400 MHz, $CDCl_3$) ppm δ = 7.09 (m, *meta*- and *para*-, 3H), 6.58 (m, *ortho*-, 2H), 1.86 (m, -CH_2, 1H) and 1.43 (m, -CH, 1H).

Azido-Terminated PS

Bromo-capped polystyrene (1.34 g, 0.088 mmol), NaN_3 (0.11 g, 1.75 mmol) and tetrabutylammonium bromide (0.56g 1.75 mmol) were dissolved in THF (8 mL) and stirred for 2 days at 40 °C. The product was precipitated from THF into MeOH (3 times). Yield: 1.26 g (94 %). M_n 15,070 Da, M_w 17,040 Da, $Đ$ = 1.13 (GPC). ^{1}H-NMR (400 MHz, $CDCl_3$) ppm δ = 7.09 (m, *meta*- and *para*-, 3H), 6.58 (m, *ortho*-, 2H), 1.86 (m, -CH_2, 1H) and 1.43 (m, -CH, 1H).

P3DSe$_{17}$-*b*-PS$_{140}$

Alkyne-capped polyselenophene (30 mg, 0.007 mol) and azido-capped polystyrene (120 mg, 0.008 mol) and PMDETA (7.47 μl , 0.014 mol) were dissolved in THF. 3 freeze-pump-thaw cycles were used to degas the solvent before CuBr (ca. 10 mg) was added. The reaction was allowed to stir for 2 days at 40 °C before being passed through a plug of basic alumina to

remove the copper salts. The material was precipitated from THF into MeOH 3 times before unreacted homopolymers were removed by sequential SEC columns. M_n 24,080 Da, M_w 27,070 Da, $Đ$ =1.12 (GPC). ^{1}H-NMR (400 MHz, $CDCl_3$) ppm δ = 7.08 (m, selenophene aromatic and *meta*- and *para*-), 6.57 (m, *ortho*-), 2.73 (t, J = 7 Hz, selenophene methylene), 1.84 (m, styrene CH_2), 1.42 (m, styrene -CH), 1.28 (m, selenophene alkyl) and 0.88 (t, J = 7 Hz, selenophene terminal alkyl).

Seeded-growth of P3DSe$_{17}$-*b*-PDMS$_{240}$ from sonicated seeds in EtOAc

The long (> 1 μm) P3DSe$_{17}$-*b*-PDMS$_{240}$ micelles were prepared by suspending the BCP in EtOAc (0.5 mg/mL) in a sealed vial and heating the solution to 70 °C in a heating block for 1 h before cooling slowly (ca. 1 °C min^{-1}) to room temperature (23 °C). The micelle solution was aged for 24 h before drop-casting an aliquot onto a carbon-coated copper grid for TEM analysis. Short (ca. 20 nm) P3DSe$_{17}$-*b*-PDMS$_{240}$ seeds were prepared from the long micelles (0.5 mg/mL in EtOAc) by subjecting the solution to ultrasonication in a cleaning bath for 1 h at 0 °C. The sample was immediately drop-cast onto a carbon-coated copper grid for TEM analysis. Seeded-growth was performed by diluting aliquots of the seeds in EtOAc (25 μL) with various volumes of EtOAc to give micelle solutions of consistent concentrations in EtOAc (0.5 mg/mL) after unimer addition. P3DSe$_{17}$-*b*-PDMS$_{240}$ unimer was added in THF (m_{unimer}/m_{seed} = 1 to 16, 1 mg/mL) to the seeds in EtOAc. The seeded-growth solutions were aged overnight prior to drop-casting aliquots onto carbon-coated copper grids for TEM analysis.

Self-assembly of P3DSe$_{17}$-*b*-PDMS$_{240}$ in Et$_2$O

P3DSe$_{17}$-*b*-PDMS$_{240}$ BCP (0.25 mg) was suspended in Et$_2$O (0.5 mL) at room temperature (23 °C). The resulting mixture was left to stand for 24 h at room temperature without stirring. TEM analysis showed the formation of short, low dispersity fibers (L_n = 41 nm, L_w/L_n = 1.16)

which were subsequently used as seeds for living CDSA. The L_n values for the seeds obtained via this method were typically in the range of 30 – 60 nm with $L_w/L_n < 1.20$.

Seeded growth of P3DSe$_{17}$-*b*-PDMS$_{240}$ in EtOAc using seeds formed in Et$_2$O

To four separate 1.5 mL screw cap vials was added 20 µL of a 0.5 mg/mL solution of seed micelles (10 µg, L_n = 41 nm, L_w/L_n = 1.16) and varying amounts of EtOAc (0.2-1.0 mL) and THF (25-0 µL) in order to adjust the THF content to 20% (v/v). To these solutions was added 25 µg, 75 µg, 150 µg, and 250 µg of P3DSe$_{17}$-*b*-PDMS$_{240}$ BCP dissolved in THF (1 mg/mL). After shaking the vial for 5 s, the solutions were aged for 48 h at room temperature (23 °C). Multiple TEM images were obtained and the contour lengths of 200 – 250 micelles were measured.

Preparation of B-A-B block co-micelles

To a 1.5 mL screw cap vials was added 100 µL of a 0.22 mg/mL solution of P3DSe$_{17}$-*b*-PDMS$_{240}$ fibers (22 µg, L_n = 389 nm, L_w/L_n = 1.10) in EtOAc containing 20% THF. To this solution was added EtOAc (88 µL) followed by 22 µg of P3DSe$_{17}$-*b*-PS$_{140}$ dissolved in THF (1 mg/mL). After agitating the vial for 5 s, the solutions were aged for 48 h at 23℃.

Acknowledgements

The authors thank the Engineering and Physical Sciences Research Council (EPSRC) for financial support.

References

(1) Mai, Y.; Eisenberg, A. Self-Assembly of Block Copolymers. *Chem. Soc. Rev.* **2012**, *41*, 5969–5985.

(2) Schacher, F. H.; Rupar, P. A.; Manners, I. Functional Block Copolymers: Nanostructured Materials with Emerging Applications. *Angew. Chemie Int. Ed.* **2012**,

51, 7898–7921.

(3) Tritschler, U.; Pearce, S.; Gwyther, J.; Whittell, G. R.; Manners, I. 50th Anniversary Perspective: Functional Nanoparticles from the Solution Self-Assembly of Block Copolymers. *Macromolecules* **2017**, *50*, 3439–3463.

(4) Elsabahy, M.; Wooley, K. L. Design of Polymeric Nanoparticles for Biomedical Delivery Applications. *Chem. Soc. Rev.* **2012**, *41*, 2545–2561.

(5) Warren, N. J.; Armes, S. P. Polymerization-Induced Self-Assembly of Block Copolymer Nano-Objects via RAFT Aqueous Dispersion Polymerization. *J. Am. Chem. Soc.* **2014**, *136*, 10174–10185.

(6) Gröschel, A. H.; Müller, A. H. E. Self-Assembly Concepts for Multicompartment Nanostructures. *Nanoscale* **2015**, *7*, 11841–11876.

(7) Gilroy, J. B.; Gädt, T.; Whittell, G. R.; Chabanne, L.; Mitchels, J. M.; Richardson, R. M.; Winnik, M. A.; Manners, I. Monodisperse Cylindrical Micelles by Crystallization-Driven Living Self-Assembly. *Nat. Chem.* **2010**, *2*, 566–570.

(8) Petzetakis, N.; Dove, A. P.; O'Reilly, R. K. Cylindrical Micelles from the Living Crystallization-Driven Self-Assembly of Poly(lactide)-Containing Block Copolymers. *Chem. Sci.* **2011**, *2*, 955.

(9) Schmelz, J.; Schedl, A. E.; Steinlein, C.; Manners, I.; Schmalz, H. Length Control and Block-Type Architectures in Worm-like Micelles with Polyethylene Cores. *J. Am. Chem. Soc.* **2012**, *134*, 14217–14225.

(10) Wang, X.; Guerin, G.; Wang, H.; Wang, Y.; Manners, I.; Winnik, M. A. Cylindrical Block Copolymer Micelles and Co-Micelles of Controlled Length and Architecture. *Science* **2007**, *317*, 644–647.

(11) Hudson, Z. M.; Lunn, D. J.; Winnik, M. A.; Manners, I. Colour-Tunable Fluorescent Multiblock Micelles. *Nat. Commun.* **2014**, *5*, 3372.

(12) Arno, M. C.; Inam, M.; Coe, Z.; Cambridge, G.; Macdougall, L. J.; Keogh, R.; Dove, A. P.; O'Reilly, R. K. Precision Epitaxy for Aqueous 1D and 2D Poly(ε-Caprolactone) Assemblies. *J. Am. Chem. Soc.* **2017**, *139*, 16980–16985.

(13) Hudson, Z. M.; Boott, C. E.; Robinson, M. E.; Rupar, P. A.; Winnik, M. A.; Manners, I. Tailored Hierarchical Micelle Architectures Using Living Crystallization-Driven Self-Assembly in Two Dimensions. *Nat. Chem.* **2014**, *6*, 893–898.

(14) Yu, B.; Jiang, X.; Yin, J. Size-Tunable Nanosheets by the Crystallization-Driven 2D Self-Assembly of Hyperbranched Poly(ether Amine) (hPEA). *Macromolecules* **2014**, *47*, 4761–4768.

(15) Qiu, H.; Gao, Y.; Boott, C. E.; Gould, O. E. C.; Harniman, R. L.; Miles, M. J.; Webb, S. E. D.; Winnik, M. A.; Manners, I. Uniform Patchy and Hollow Rectangular Platelet Micelles from Crystallizable Polymer Blends. *Science* **2016**, *352*, 697–701.

(16) Ganda, S.; Dulle, M.; Drechsler, M.; Förster, B.; Förster, S.; Stenzel, M. H. Two-Dimensional Self-Assembled Structures of Highly Ordered Bioactive Crystalline-Based Block Copolymers. *Macromolecules* **2017**, *50*, 8544–8553.

(17) Zhang, W.; Jin, W.; Fukushima, T.; Saeki, A.; Seki, S.; Aida, T. Supramolecular Linear Heterojunction Composed of Graphite-like Semiconducting Nanotubular Segments. *Science* **2011**, *334*, 340–343.

(18) Ogi, S.; Sugiyasu, K.; Manna, S.; Samitsu, S.; Takeuchi, M. Living Supramolecular Polymerization Realized through a Biomimetic Approach. *Nat. Chem.* **2014**, *6*, 188–195.

(19) Ogi, S.; Stepanenko, V.; Sugiyasu, K.; Takeuchi, M.; Würthner, F. Mechanism of Self-Assembly Process and Seeded Supramolecular Polymerization of Perylene Bisimide Organogelator. *J. Am. Chem. Soc.* **2015**, *137*, 3300–3307.

(20) Robinson, M. E.; Lunn, D. J.; Nazemi, A.; Whittell, G. R.; De Cola, L.; Manners, I. Length Control of Supramolecular Polymeric Nanofibers Based on Stacked Planar Platinum(II) Complexes by Seeded-Growth. *Chem. Commun.* **2015**, *51*, 15921–15924.

(21) Bu, L.; Dawson, T. J.; Hayward, R. C. Tailoring Ultrasound-Induced Growth of Perylene Diimide Nanowire Crystals from Solution by Modification with Poly(3-Hexyl Thiophene). *ACS Nano* **2015**, *9*, 1878–1885.

(22) Ma, X.; Zhang, Y.; Zhang, Y.; Liu, Y.; Che, Y.; Zhao, J. Fabrication of Chiral-Selective Nanotubular Heterojunctions through Living Supramolecular Polymerization. *Angew. Chemie Int. Ed.* **2016**, *55*, 9539–9543.

(23) Fukui, T.; Kawai, S.; Fujinuma, S.; Matsushita, Y.; Yasuda, T.; Sakurai, T.; Seki, S.; Takeuchi, M.; Sugiyasu, K. Control over Differentiation of a Metastable Supramolecular Assembly in One and Two Dimensions. *Nat. Chem.* **2016**, *9*, 493–499.

(24) Greciano, E. E.; Sánchez, L. Seeded Supramolecular Polymerization in a Three-Domain Self-Assembly of an N-Annulated Perylenetetracarboxamide. *Chem. Eur. J.* **2016**, *22*, 13724–13730.

(25) Aliprandi, A.; Mauro, M.; De Cola, L. Controlling and Imaging Biomimetic Self-Assembly. *Nat. Chem.* **2015**, *8*, 10–15.

(26) Günes, S.; Neugebauer, H.; Sariciftci, N. S. Conjugated Polymer-Based Organic Solar Cells. *Chem. Rev.* **2007**, *107*, 1324–1338.

(27) Shrotriya, V. Organic Photovoltaics: Polymer Power. *Nat. Photonics* **2009**, *3*, 447–

449.

(28) Kempf, C. N.; Smith, K. A.; Pesek, S. L.; Li, X.; Verduzco, R. Amphiphilic Poly(alkylthiophene) Block Copolymers Prepared via Externally Initiated GRIM and Click Coupling. *Polym. Chem.* **2013**, *4*, 2158.

(29) Kamps, A. C.; Cativo, M. H. M.; Fryd, M.; Park, S. J. Self-Assembly of Amphiphilic Conjugated Diblock Copolymers into One-Dimensional Nanoribbons. *Macromolecules* **2014**, *47*, 161–164.

(30) Wang, H.; Wang, H. H.; Urban, V. S.; Littrell, K. C.; Thiyagarajan, P.; Yu, L. Syntheses of Amphiphilic Diblock Copolymers Containing a Conjugated Block and Their Self-Assembling Properties. *J. Am. Chem. Soc.* **2000**, *122*, 6855–6861.

(31) Kim, Y. J.; Cho, C. H.; Paek, K.; Jo, M.; Park, M. K.; Lee, N. E.; Kim, B. J.; Lee, E. Precise Control of Quantum Dot Location within the P3HT-B-P2VP/QD Nanowires Formed by Crystallization-Driven 1D Growth of Hybrid Dimeric Seeds. *J. Am. Chem. Soc.* **2014**, *136*, 2767–2774.

(32) Lee, E.; Hammer, B.; Kim, J.-K.; Page, Z.; Emrick, T.; Hayward, R. C. Hierarchical Helical Assembly of Conjugated Poly(3-Hexylthiophene)-Block-poly(3-Triethylene Glycol Thiophene) Diblock Copolymers. *J. Am. Chem. Soc.* **2011**, *133*, 10390–10393.

(33) Yang, S.; Shin, S.; Choi, I.; Lee, J.; Choi, T.-L. Direct Formation of Large-Area 2D Nanosheets from Fluorescent Semiconducting Homopolymer with Orthorhombic Crystalline Orientation. *J. Am. Chem. Soc.* **2017**, *139*, 3082–3088.

(34) Cativo, M. H. M.; Kim, D. K.; Riggleman, R. A.; Yager, K. G.; Nonnenmann, S. S.; Chao, H.; Bonnell, D. A.; Black, C. T.; Kagan, C. R.; Park, S.-J. Air–Liquid Interfacial Self-Assembly of Conjugated Block Copolymers into Ordered Nanowire Arrays. *ACS*

Nano **2014**, *8*, 12755–12762.

(35) Lee, I.-H.; Amaladass, P.; Yoon, K.-Y.; Shin, S.; Kim, Y.-J.; Kim, I.; Lee, E.; Choi, T.-L. Nanostar and Nanonetwork Crystals Fabricated by in Situ Nanoparticlization of Fully Conjugated Polythiophene Diblock Copolymers. *J. Am. Chem. Soc.* **2013**, *135*, 17695–17698.

(36) Park, S. J.; Kang, S. G.; Fryd, M.; Saven, J. G. Highly Tunable Photoluminescent Properties of Amphiphilic Conjugated Block Copolymers. *J. Am. Chem. Soc.* **2010**, *132*, 9931–9933.

(37) Ren, G.; Wu, P.-T.; Jenekhe, S. A. Solar Cells Based on Block Copolymer Semiconductor Nanowires: Effects of Nanowire Aspect Ratio. *ACS Nano* **2011**, *5*, 376–384.

(38) Jin, S.-M.; Kim, I.; Lim, J. A.; Ahn, H.; Lee, E. Interfacial Crystallization-Driven Assembly of Conjugated Polymers/Quantum Dots into Coaxial Hybrid Nanowires: Elucidation of Conjugated Polymer Arrangements by Electron Tomography. *Adv. Funct. Mater.* **2016**, *26*, 3226–3235.

(39) Lohwasser, R. H.; Thelakkat, M. Synthesis of Amphiphilic Rod–Coil P3HT- B -P4VP Carrying a Long Conjugated Block Using NMRP and Click Chemistry. *Macromolecules* **2012**, *45*, 3070–3077.

(40) Cui, H.; Yang, X.; Peng, J.; Qiu, F. Controlling the Morphology and Crystallization of a Thiophene-Based All-Conjugated Diblock Copolymer by Solvent Blending. *Soft Matter* **2017**, *13*, 5261–5268.

(41) Patra, S. K.; Ahmed, R.; Whittell, G. R.; Lunn, D. J.; Dunphy, E. L.; Winnik, M. A.; Manners, I. Cylindrical Micelles of Controlled Length with a π-Conjugated

Polythiophene Core via Crystallization-Driven Self-Assembly. *J. Am. Chem. Soc.* **2011**, *133*, 8842–8845.

(42) Gwyther, J.; Gilroy, J. B.; Rupar, P. A.; Lunn, D. J.; Kynaston, E.; Patra, S. K.; Whittell, G. R.; Winnik, M. A.; Manners, I. Dimensional Control of Block Copolymer Nanofibers with a π-Conjugated Core: Crystallization-Driven Solution Self-Assembly of Amphiphilic Poly(3-Hexylthiophene)-B-poly(2-Vinylpyridine). *Chem. Eur. J.* **2013**, *19*, 9186–9197.

(43) Qian, J.; Li, X.; Lunn, D. J.; Gwyther, J.; Hudson, Z. M.; Kynaston, E.; Rupar, P. A.; Winnik, M. A.; Manners, I. Uniform, High Aspect Ratio Fiber-like Micelles and Block Co-Micelles with a Crystalline π-Conjugated Polythiophene Core by Self-Seeding. *J. Am. Chem. Soc.* **2014**, *136*, 4121–4124.

(44) Tao, D.; Feng, C.; Cui, Y.; Yang, X.; Manners, I.; Winnik, M. A.; Huang, X. Monodisperse Fiber-like Micelles of Controlled Length and Composition with an Oligo(p-Phenylenevinylene) Core via "Living" Crystallization-Driven Self-Assembly. *J. Am. Chem. Soc.* **2017**, *139*, 7136–7139.

(45) Li, X.; Wolanin, P. J.; MacFarlane, L. R.; Harniman, R. L.; Qian, J.; Gould, O. E. C.; Dane, T. G.; Rudin, J.; Cryan, M. J.; Schmaltz, T.; *et al.* Uniform Electroactive Fibre-like Micelle Nanowires for Organic Electronics. *Nat. Commun.* **2017**, *8*, 15909.

(46) Patra, A.; Bendikov, M. Polyselenophenes. *J. Mater. Chem.* **2010**, *20*, 422–433.

(47) Heeney, M.; Zhang, W.; Crouch, D. J.; Chabinyc, M. L.; Gordeyev, S.; Hamilton, R.; Higgins, S. J.; McCulloch, I.; Skabara, P. J.; Sparrowe, D.; *et al.* Regioregular poly(3-Hexyl)selenophene: A Low Band Gap Organic Hole Transporting Polymer. *Chem. Commun.* **2007**, 5061.

(48) Yan, H.; Hollinger, J.; Bridges, C. R.; McKeown, G. R.; Al-Faouri, T.; Seferos, D. S. Doping Poly(3-Hexylthiophene) Nanowires with Selenophene Increases the Performance of Polymer-Nanowire Solar Cells. *Chem. Mater.* **2014**, *26*, 4605–4611.

(49) Li, L.; Hollinger, J.; Jahnke, A. A.; Petrov, S.; Seferos, D. S. Polyselenophenes with Distinct Crystallization Properties. *Chem. Sci.* **2011**, *2*, 2306.

(50) Kynaston, E. L.; Gould, O. E. C.; Gwyther, J.; Whittell, G. R.; Winnik, M. A.; Manners, I. Fiber-Like Micelles from the Crystallization-Driven Self-Assembly of Poly(3-Heptylselenophene)-Block-Polystyrene. *Macromol. Chem. Phys.* **2015**, *216*, 685–695.

(51) Hollinger, J.; Sun, J.; Gao, D.; Karl, D.; Seferos, D. S. Statistical Conjugated Polymers Comprising Optoelectronically Distinct Units. *Macromol. Rapid Commun.* **2013**, *34*, 437–441.

(52) Hollinger, J.; Seferos, D. S. Morphology Control of Selenophene–Thiophene Block Copolymers through Side Chain Engineering. *Macromolecules* **2014**, *47*, 5002–5009.

(53) Al-Hashimi, M.; Baklar, M. A.; Colleaux, F.; Watkins, S. E.; Anthopoulos, T. D.; Stingelin, N.; Heeney, M. Synthesis, Characterization, and Field Effect Transistor Properties of Regioregular Poly(3-Alkyl-2,5-Selenylenevinylene). *Macromolecules* **2011**, *44*, 5194–5199.

(54) Jeffries-El, M.; Sauvé, G.; McCullough, R. D. Facile Synthesis of End-Functionalized Regioregular Poly(3-Alkylthiophene)s via Modified Grignard Metathesis Reaction. *Macromolecules* **2005**, *38*, 10346–10352.

(55) Zade, S. S.; Zamoshchik, N.; Bendikov, M. Oligo- and Polyselenophenes: A Theoretical Study. *Chem. Eur. J.* **2009**, *15*, 8613–8624.

(56) Prosa, T. J.; Winokur, M. J.; Moulton, J.; Smith, P.; Heeger, A. J. X-Ray Structural Studies of poly(3-Alkylthiophenes): An Example of an Inverse Comb. *Macromolecules* **1992**, *25*, 4364–4372.

(57) Prosa, T. J.; Winokur, M. J.; McCullough, R. D. Evidence of a Novel Side Chain Structure in Regioregular poly(3-Alkylthiophenes). *Macromolecules* **1996**, *29*, 3654–3656.

(58) McCulloch, B.; Ho, V.; Hoarfrost, M.; Stanley, C.; Do, C.; Heller, W. T.; Segalman, R. A. Polymer Chain Shape of poly(3-Alkylthiophenes) in Solution Using Small-Angle Neutron Scattering. *Macromolecules* **2013**, *46*, 1899–1907.

(59) Surin, M.; Coulembier, O.; Tran, K.; Winter, J. De; Leclère, P.; Gerbaux, P.; Lazzaroni, R.; Dubois, P. Regioregular poly(3-Hexylthiophene)-Poly(ε-Caprolactone) Block Copolymers: Controlled Synthesis, Microscopic Morphology, and Charge Transport Properties. *Org. Electron.* **2010**, *11*, 767–774.

(60) Xu, B.; Holdcroft, S. Molecular Control of Luminescence from Poly(3-Hexylthiophenes). *Macromolecules* **1993**, *26*, 4457–4460.

(61) Qian, J.; Lu, Y.; Chia, A.; Zhang, M.; Rupar, P. A.; Gunari, N.; Walker, G. C.; Cambridge, G.; He, F.; Guerin, G.; *et al.* Self-Seeding in One Dimension: A Route to Uniform Fiber-like Nanostructures from Block Copolymers with a Crystallizable Core-Forming Block. *ACS Nano* **2013**, *7*, 3754–3766.

(62) Qian, J.; Guerin, G.; Lu, Y.; Cambridge, G.; Manners, I.; Winnik, M. A. Self-Seeding in One Dimension: An Approach To Control the Length of Fiberlike Polyisoprene-Polyferrocenylsilane Block Copolymer Micelles. *Angew. Chemie Int. Ed.* **2011**, *50*, 1622–1625.

(63) Gilroy, J. B.; Lunn, D. J.; Patra, S. K.; Whittell, G. R.; Winnik, M. A.; Manners, I. Fiber-like Micelles via the Crystallization-Driven Solution Self-Assembly of Poly(3-Hexylthiophene)-Block-Poly(methyl Methacrylate) Copolymers. *Macromolecules* **2012**, *45*, 5806–5815.

(64) Lazzari, M.; Scalarone, D.; Vazquez-Vazquez, C.; López-Quintela, M. A. Cylindrical Micelles from the Self-Assembly of Polyacrylonitrile-Based Diblock Copolymers in Nonpolar Selective Solvents. *Macromol. Rapid Commun.* **2008**, *29*, 352–357.

(65) Schmelz, J.; Karg, M.; Hellweg, T.; Schmalz, H. General Pathway toward Crystalline-Core Micelles with Tunable Morphology and Corona Segregation. *ACS Nano* **2011**, *5*, 9523–9534.

(66) Massey, J. A.; Temple, K.; Cao, L.; Rharbi, Y.; Raez, J.; Winnik, M. A.; Manners, I. Self-Assembly of Organometallic Block Copolymers: The Role of Crystallinity of the Core-Forming Polyferrocene Block in the Micellar Morphologies Formed by Poly(ferrocenylsilane-B-Dimethylsiloxane) in N-Alkane Solvents. *J. Am. Chem. Soc.* **2000**, *122*, 11577–11584.

(67) Guerin, G.; Wang, H.; Manners, I.; Winnik, M. A. Fragmentation of Fiberlike Structures: Sonication Studies of Cylindrical Block Copolymer Micelles and Behavioral Comparisons to Biological Fibrils. *J. Am. Chem. Soc.* **2008**, *130*, 14763–14771.